Explicit analytic prediction for hydrogen-oxygen ignition times at temperatures below crossover.

P. Boivin[a], A. L. Sánchez[a], F.A. Williams[b]

[a]*Dept. Ingeniería Térmica y de Fluidos, Universidad Carlos III de Madrid, Leganés 28911, Spain*
[b]*Dept. of Mechanical and Aerospace Engineering, University of California San Diego, La Jolla CA 92093-0411, USA*

Abstract

This paper addresses homogeneous ignition of hydrogen-oxygen mixtures when the initial conditions of temperature and pressure place the system below the crossover temperature associated with the second explosion limit. A three-step reduced mechanism involving H_2, O_2, H_2O, H_2O_2 and HO_2, derived previously from a skeletal mechanism of eight elementary steps by assuming O, OH and H to follow steady state, is seen to describe accurately the associated thermal explosion. At sufficiently low temperatures, HO_2 consumption through $HO_2 + HO_2 \rightarrow H_2O_2 + O_2$ is fast enough to place this intermediate in steady state after a short build-up period, thereby reducing further the chemistry description to the two global steps $2H_2 + O_2 \rightarrow 2H_2O$ and $2H_2O \rightarrow H_2O_2 + H_2$. The strong temperature sensitivity of the corresponding overall rates enables activation-energy asymptotics to be used in describing the resulting thermal runaway, yielding an explicit expression that predicts with excellent accuracy the ignition time for different conditions of initial temperature, composition, and pressure.

Key words: hydrogen ignition, reduced chemistry, induction time, crossover temperature, activation-energy asymptotics

1. Introduction

Hydrogen-oxygen autoignition is of interest because of applications in hypersonic air-breathing propulsion, reliable performance of gas-turbine mixing systems, and safety issues associated with planning of a future hydrogen economy. The ignition time t_i appears as a key quantity, with knowledge of dependences on temperature, pressure, and composition being of utmost importance. Experimental measurements in shock-tube facilities and flow reactors as well as numerical computations of homogeneous adiabatic ignition histories have demonstrated a strong influence of the initial temperature on the ignition history, with ignition times changing rapidly as the so-called crossover temperature is approached, at which the effective rate of the $H+O_2$ branching step becomes equal to the rate of the $H+O_2+M$ recombination step.

Numerous analytic studies of ignition above crossover are available, including explicit analytic predictions of induction times [1]–[7]. By way of contrast, theoretical investigations of low-temperature ignition are scarce. The most notable contribution is that of Treviño [6], who identified in particular the key chemistry and attempted an analysis of the corresponding ignition event. He found in particular that, while H_2-O_2 ignition at high temperature takes place as a branched-chain explosion, a thermal runaway characterizes ignition below crossover. The present contribution extends the previous work by further simplifying the chemistry description to a form that is amenable to asymptotic treatment by activation-energy asymptotics, leading to an explicit expression that gives predictions of induction times in close agreement with those obtained by numerical integrations employing detailed chemistry.

Before proceeding with the analysis, it is worth mentioning that exper-

iments of homogeneous ignition encounter numerous difficulties at temperatures below crossover [8], with ignition occuring locally at points typically located near walls and extending to the reactive mixture through flame propagation. As a result, the ignition delay measured experimentally in shock tubes is not that corresponding to homogeneous autoignition but rather the ratio of the tube radius to the flame speed [9]. Although more work is required to further clarify the nature of these low-temperature shock-tube processes, that is not the intention of the present paper. Instead, the analysis focuses on the homogeneous ignition regime by taking a widely accepted, detailed chemical-kinetic mechanism [10] as a starting point for the development of analytical results and using this detailed scheme in numerical integrations for validation purposes.

2. Reduced-Chemistry Description

At sufficiently high temperature, ignition is characterized by a long induction period of chain-carrier growth determined by the competition of chain-branching reactions, such as $H+O_2 \xrightarrow{1} OH+O$, with chain-terminating three-body collisions, such as $H+O_2+M \xrightarrow{4} HO_2+M$, while the initiation reaction $H_2+O_2 \xrightarrow{5} HO_2+H$ is only significant during the initial instants. If the mixture is sufficiently rich, then the shuffle reactions $H_2+O \xrightarrow{2} OH+H$ and $H_2+OH \xrightarrow{3} H_2O+H$ are sufficiently fast for the radicals O and OH to maintain steady state. In that case, a single global reaction of the form $3H_2+O_2 \rightarrow 2H_2O+2H$ describes accurately the growth of H radicals, the rate of H-atom production being given by twice that of reaction 1 minus that of reaction 4 [7].

Previous theoretical analyses have shown that high-temperature ignition histories can be computed accurately from integrations of unsteady homogeneous equations in isobaric adiabatic systems, which yield analytic expres-

sions for the induction time above crossover when the effects of reactant consumption and heat release are both neglected during the induction period [1]–[7]. Ignition events described by the overall reaction $3H_2+O_2 \rightarrow 2H_2O+2H$ have ignition times t_i that increase linearly proportional to $(2k_1 - k_4 C_{M_4})^{-1}$, where k_j represents the rate constant for reaction j and C_{M_4} is the effective third-body concentration of reaction 4. This factor defines the relevant crossover temperature for ignition of rich mixtures according to $2k_1 = k_4 C_{M_4}$, giving a value on the order of $T_c = 950$ K at atmospheric pressure. For temperatures above crossover, the inequality $2k_1 > k_4 C_{M_4}$ applies and a successful branched-chain explosion develops. As the temperature decreases, chain termination through $H+O_2+M \overset{4}{\rightarrow} HO_2+M$ becomes increasingly important, augmenting the induction time and causing the prediction for t_i to diverge to infinity as crossover is reached [7].

Clearly, the prevailing rate of chain termination through $H+O_2+M \overset{4}{\rightarrow} HO_2+M$ precludes in principle chain branching at temperatures below crossover. As shown by Treviño [6], the alternative branched-chain path that enables ignition is provided by $H_2O_2+M \overset{8}{\rightarrow} 2OH+M$, with H_2O_2 being formed through $2HO_2 \overset{6}{\rightarrow} H_2O_2+O_2$ and, to a smaller extent, also through $HO_2+H_2 \overset{7}{\rightarrow} H_2O_2+H$, so that a total of 8 elementary reactions, shown in Table 1, are needed for the description of low-temperature ignition. The reaction-rate parameters included in the table are those of the so-called San-Diego mechanism [10], a detailed 21-step scheme that will be used below in the numerical integrations for validation purposes.

Treviño also noticed that, because of rapid H-atom removal through $H+O_2+M \overset{4}{\rightarrow} HO_2+M$, all three radicals O, OH and H maintain steady state during ignition below crossover [6]. The resulting reduced chemistry can be

expressed as three overall steps

$$\begin{aligned} 2H_2 + O_2 &\overset{\text{I}}{\rightarrow} 2H_2O \\ 2H_2O &\overset{\text{II}}{\rightarrow} H_2O_2 + H_2 \\ H_2 + 2O_2 &\overset{\text{III}}{\rightarrow} 2HO_2 \end{aligned}$$

with rates (mols per unit volume per unit time) given by $\omega_{\text{I}} = w_1 + w_6 + w_7$, $\omega_{\text{II}} = w_6 + w_7 - w_8$, and $\omega_{\text{III}} = \frac{1}{2}(w_4 + w_5 - 2w_6 - w_7)$, and with the H-atom concentration, needed to evaluate w_1 and w_4, given by its steady-state expression

$$C_{\text{H}} = \frac{w_5 + w_7 + 2w_8}{(k_4 C_{\text{M}_4} - 2k_1) C_{\text{O}_2}}. \tag{1}$$

Results obtained by using this three-step mechanism in numerical integrations of adiabatic, isobaric homogeneous reactors are compared in Fig. 1 with those obtained with the 21-step San Diego mechanism, with the ignition time defined in the computations by the temperature-inflection criterion. For the stoichiometric H_2-air mixture considered, the crossover temperature defined from the condition $2k_1 = k_4 C_{\text{M}_4}$ is $T_c = (943, 1186, 1431)$ K for $p = (1, 10, 50)$ atm. As can be seen, Treviño's chemistry gives excellent agreement for the three pressures tested in the figure for initial temperatures below the crossover value. Since it is evident from (1) that the reduction fails at crossover, it is noteworthy that the results remain reasonable up to within about 25 K of crossover.

3. Further Chemistry Simplifications

The thermal-explosion character of ignition at temperatures below crossover is illustrated in the plot of Fig. 2, which shows the temperature evolution for a stoichiometric H_2-air mixture at atmospheric pressure and with initial temperature $T = 820$ K. The very sharp temperature increase after the long delay

involving an imperceptible temperature rise is indicative of a thermal explosion. To investigate the steady state of HO_2 and H_2O_2, the plot also includes as dashed curves the evolution with time of the ratio $(w_p - w_c)/w_p$ for these two species prior to ignition, with w_p and w_c representing their production and consumption rates (e.g., for HO_2, $w_p = w_4 + w_5$ and $w_c = 2w_6 + w_7$). As can be seen, a steady-state assumption is never a good approximation for H_2O_2. On the other hand, the HO_2 balance indicates that there exists an initial period in which this intermediate is created with negligible consumption, through H_2+$O_2 \stackrel{5}{\rightarrow} HO_2$+H followed by H+$O_2$+M $\stackrel{4}{\rightarrow} HO_2$+M. When the HO_2 concentration reaches a sufficiently large value the overall consumption rate $2w_6 + w_7$ becomes significant and eventually places this intermediate in steady state. Consequently, the HO_2 steady-state equation $w_4 + w_5 - 2w_6 - w_7 = 0$ applies with good accuracy over most of the ignition history, with the exception of the initial buildup period, to be neglected in the following description. This last steady-state equation, together with that of the H-atom, given in (1), yields

$$\begin{aligned} \omega_{\rm I} &= \frac{w_5 + w_7 + (1+\alpha)w_8}{1-\alpha} \\ \omega_{\rm II} &= \frac{(1-\frac{1}{2}\alpha)(w_5 + w_7) + \alpha w_8}{1-\alpha}, \end{aligned} \tag{2}$$

for the rates of the overall steps

$$\begin{aligned} 2H_2 + O_2 &\stackrel{\rm I}{\rightarrow} 2H_2O \\ 2H_2O &\stackrel{\rm II}{\rightarrow} H_2O_2 + H_2. \end{aligned} \tag{3}$$

The reaction-rate ratio $\alpha = 2k_1/(k_4 C_{M_4})$ appearing above, which equals unity at crossover, decreases rapidly as the temperature decreases, reaching values

on the order of $\alpha \sim 0.05$ as the temperature falls 200 K below crossover. The HO_2 concentration, needed to compute w_7, can be determined from the truncated expression

$$C_{HO_2} = \left(\frac{(2-\alpha)w_5 + 2w_8}{2(1-\alpha)k_6} \right)^{1/2}, \tag{4}$$

obtained from the corresponding steady-state equation $w_4+w_5-2w_6-w_7 = 0$ by using (1) to write w_4 and neglecting hydroperoxyl consumption through $HO_2 + H_2 \xrightarrow{7} H_2O_2 + H$, an excellent approximation under most conditions.

The accuracy of the 2-step mechanism is tested in Fig. 1, in which the initial concentrations involve no radicals for the detailed chemistry but very small radical concentrations consistent with the steady states for the reduced mechanisms. As can be seen, the agreement obtained is excellent for initial temperatures $T \lesssim 1000$ K, including in particular all temperatures below crossover at atmospheric pressure. Increasing departures are however observed for higher temperatures in the plots for $p = 10$ atm and $p = 50$ atm. At these elevated temperatures, ignition times are short, because H_2O_2 consumption through reaction 8 becomes very fast. Since the HO_2 chemistry is much less dependent on temperature changes, as can be seen in the reaction-rate constants of $H+O_2+M \xrightarrow{4} HO_2+M$ and $2HO_2 \xrightarrow{6} H_2O_2+O_2$, the steady-state assumption for this species becomes less accurate, in that the initial HO_2 build-up period, required for the HO_2 concentration to increase to a sufficiently large value for its steady state to apply, takes up a significant fraction of the total ignition delay time. When that occurs, the 2-step mechanism becomes less accurate and leads, for instance, to underpredictions in ignition time of the order of 50% for $p = 50$ atm and $T = 1200$ K. Except at those high-pressure, high-temperature conditions, the degree of accuracy of the 2-step mechanism exhibited in Fig. 1 is quite satisfactory, thereby motivating the following development.

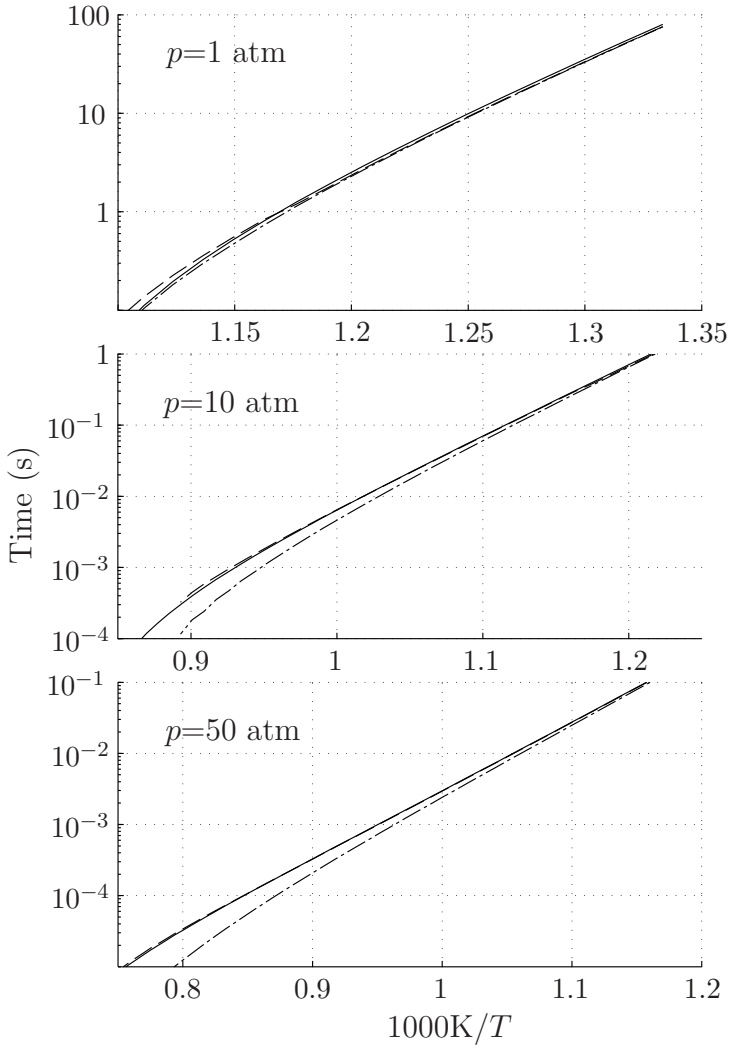

Figure 1: Ignition time obtained for a stoichiometric H_2-air mixture with 21-step detailed chemistry (solid line), with Treviño's 3-step reduced mechanism (dashed curves), and with the 2-step reduced mechanism given in (3) with the truncated HO_2 expression (4) (dot-dashed curves).

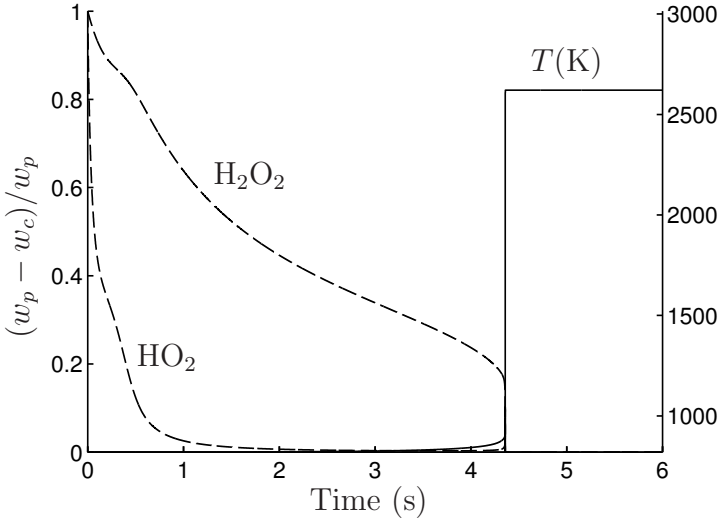

Figure 2: The temperature evolution (solid curve) during ignition of a stoichiometric H_2-air mixture at atmospheric pressure and with initial temperature $T = 820$ K. The dashed curves represent the corresponding steady-state ratios $(w_p - w_c)/w_p$ for HO_2 and H_2O_2 prior to ignition, with w_p and w_c representing their production and consumption rates.

4. Activation-Energy Asymptotics

With reactant consumption neglected, as is appropriate given the thermal-runaway character of the ignition, the problem of homogeneous ignition in an adiabatic isobaric reactor reduces to that of integrating

$$\begin{aligned} \frac{\mathrm{d}C_{\mathrm{H_2O_2}}}{\mathrm{d}t} &= \omega_{\mathrm{II}} \\ \rho c_p \frac{\mathrm{d}T}{\mathrm{d}t} &= -2h_{\mathrm{H_2O}}(\omega_{\mathrm{I}} - \omega_{\mathrm{II}}) - h_{\mathrm{H_2O_2}}\omega_{\mathrm{II}} \end{aligned} \tag{5}$$

with initial conditions $T - T_o = C_{\mathrm{H_2O_2}} = 0$, where ρ and c_p are the initial values of the density and specific heat at constant pressure, and $h_{\mathrm{H_2O}} = -241.8$ kJ/mol and $h_{\mathrm{H_2O_2}} = -136.11$ kJ/mol are the values of the standard enthalpy of formation of the products. The analysis can be further simplified by noting that the direct contribution of w_5 to the rates (2) is always small, initiation being triggered by w_7 through the term involving w_5 in $C_{\mathrm{HO_2}}$. Also, the combined contribution $\alpha(w_8 - \frac{1}{2}w_7)$ to ω_{II} can be neglected in the first approximation under most conditions, so that $\omega_{\mathrm{II}} \simeq w_7/(1-\alpha)$. When these additional simplifications are incorporated into (5) with (4) used to express $C_{\mathrm{HO_2}}$, the reduced expressions

$$\begin{aligned} \omega_{\mathrm{I}} - \omega_{\mathrm{II}} &= \frac{1+\alpha}{1-\alpha} k_8 C_{\mathrm{M_8}} C_{\mathrm{H_2O_2}} \\ \omega_{\mathrm{II}} &= \frac{k_7 k_8^{1/2}}{k_6^{1/2}} \frac{C_{\mathrm{H_2}} C_{\mathrm{M_8}}}{(1-\alpha)^{3/2}} \left[\left(1 - \frac{\alpha}{2}\right) \frac{k_5 C_{\mathrm{H_2}} C_{\mathrm{O_2}}}{k_8 C_{\mathrm{M_8}}^2} + \frac{C_{\mathrm{H_2O_2}}}{C_{\mathrm{M_8}}} \right]^{1/2}, \end{aligned} \tag{6}$$

are obtained for the overall rates, where $C_{\mathrm{M_8}}$ is the effective third-body concentration of reaction 8.

The activation energies of $k_7(k_8/k_6)^{1/2}$ and k_8 are very large, as could have been anticipated in view of the thermal-runaway character of the temperature

evolution in Fig. 2. Their dimensionless values can be written with account taken of the algebraic temperature dependences present in k_7 and k_8 to give for instance $\beta_7 = E_7/(R^oT_o) + n_7 + \frac{1}{2}[E_8/(R^oT_o) + n_8 - E_6/(R^oT_o)] = 29.88$ and $\beta_8 = E_8/(R^oT_o) + n_8 = 29.31$ at $T_o = 800$ K. As can be seen, differences between these two quantities are very small and can be consequently neglected in the first approximation in the following asymptotic analysis, which uses a single dimensionless activation energy $\beta = \beta_7 = \beta_8$ to define a dimensionless temperature increment

$$\theta = \beta \frac{T - T_o}{T_o}. \tag{7}$$

The resulting thermal explosion can be described by introducing additional dimensionless variables

$$\varphi = \left[(1-\alpha)^{1/2}(1+\alpha)\beta q\right]^{2/3} \left(\frac{k_7}{(k_6k_8)^{1/2}}\right)^{-2/3} \left(\frac{C_{\mathrm{H_2}}}{C_{\mathrm{M_8}}}\right)^{-2/3} \frac{C_{\mathrm{H_2O_2}}}{C_{\mathrm{M_8}}}, \tag{8}$$

and

$$\tau = \frac{(1+\alpha)^{1/3}}{(1-\alpha)^{4/3}} (\beta q)^{1/3} k_8 C_{\mathrm{M_8}} \left(\frac{k_7}{(k_6k_8)^{1/2}}\right)^{2/3} \left(\frac{C_{\mathrm{H_2}}}{C_{\mathrm{M_8}}}\right)^{2/3} t, \tag{9}$$

with

$$q = \frac{-2h_{\mathrm{H_2O}} C_{\mathrm{M_8}}}{\rho c_p T_o}, \tag{10}$$

all quantities (except, of course, $C_{\mathrm{H_2O_2}}$ and t) evaluated in the initial mixture, reducing the problem to that of integrating

$$\frac{\mathrm{d}\varphi}{\mathrm{d}\tau} = (a+\varphi)^{1/2} e^{\theta} \tag{11}$$

$$\frac{\mathrm{d}\theta}{\mathrm{d}\tau} = \varphi e^{\theta} + \Lambda (a+\varphi)^{1/2} e^{\theta} \tag{12}$$

with initial conditions $\varphi = \theta = 0$ at $\tau = 0$. In the formulation,

$$a = \left(1 - \frac{\alpha}{2}\right)^{1/3} (1-\alpha)^{1/3} (1+\alpha)^{2/3} (\beta q)^{2/3} \frac{k_5 k_6^{1/3}}{(k_7 k_8)^{2/3}} \left(\frac{C_{\mathrm{H_2}}}{C_{\mathrm{M_8}}}\right)^{1/3} \left(\frac{C_{\mathrm{O_2}}}{C_{\mathrm{M_8}}}\right) \tag{13}$$

is a parameter measuring the initiation rate and

$$\Lambda = \left[\frac{k_7/(k_6k_8)^{1/2}}{(1-\alpha)^{1/2}(1+\alpha)}\right]^{2/3} (\beta q)^{1/3} \left(\frac{C_{\mathrm{H_2}}}{C_{\mathrm{M_8}}}\right)^{2/3} \frac{h_{\mathrm{H_2O_2}}}{2h_{\mathrm{H_2O}}} \tag{14}$$

is a measure of the ratio of the heat-release rates associated with H_2O_2 and H_2O production. Note that the problem can be written as a single differential equation by dividing (11) and (12) and integrating to give

$$\theta = \frac{2}{3}(a+\varphi)^{3/2} - 2a(a+\varphi)^{1/2} + \frac{4}{3}a^{3/2} + \Lambda\varphi \tag{15}$$

which can then be substituted into (11) to give an equation for the evolution of φ with τ.

The solution can be simplified by recognizing that $a \ll 1$, with typical values being of order $a \sim 10^{-4}$ at $T = 800$ K. Initiation is only important for $\tau \sim a^{1/2}$ when $\varphi \sim \theta \sim a$, and becomes negligible at later times, when (15) reduces to $\theta = (2/3)\varphi^{3/2} + \Lambda\varphi$, so that the ignition time associated with thermal runaway is obtained from the quadrature

$$\tau_i = \int_0^\infty \frac{\mathrm{d}\varphi}{\varphi^{1/2}\exp\left(\frac{2}{3}\varphi^{3/2} + \Lambda\varphi\right)}, \tag{16}$$

which converges as $\varphi \to 0$ because of the square-root dependence $\varphi^{1/2}$ affecting the H_2O_2 production rate. Note that if a linear dependence were present instead, as is typical of chain-branching processes, careful consideration of the initiation period would have been required, complicating the analysis, as shown in the general theory of branched-chain thermal explosions [11]. As an additional simplification to (16), it should also be noted that the reat release associated with H_2O_2 production is relatively small, giving small values of $\Lambda \simeq 0.05$. If the corresponding contribution in the exponential is neglected, then the above integral reduces to $\tau_i = (2/3)^{2/3}\Gamma(1/3) \simeq 2.0444$, where Γ is the Gamma function.

5. The ignition time

With use made of (9), this final result of the activation-energy analysis can be expressed in dimensional form to yield

$$t_i = 2.0444 \frac{(1-\alpha)^{4/3}}{(1+\alpha)^{1/3}} (\beta q)^{-1/3} (k_8 C_{\mathrm{M}_8})^{-1} \left(\frac{k_7}{(k_6 k_8)^{1/2}} \right)^{-2/3} \left(\frac{C_{\mathrm{H}_2}}{C_{\mathrm{M}_8}} \right)^{-2/3} \qquad (17)$$

as a prediction for the ignition time, where all reaction-rate constants and the parameters

$$\beta = \frac{E_8}{R^o T} + n_8, \quad q = -\frac{2 h_{\mathrm{H_2O}} C_{\mathrm{M}_8}}{\rho c_p T} \quad \text{and} \quad \alpha = \frac{2 k_1}{k_4 C_{\mathrm{M}_4}} \qquad (18)$$

are to be evaluated at the initial conditions, with the chaperon efficiencies taken into account in writing the effective third-body concentrations $C_{\mathrm{M}_4} = p(1+1.5X_{\mathrm{H}_2}+15X_{\mathrm{H_2O}})/(R^o T)$ and $C_{\mathrm{M}_8} = p(1+X_{\mathrm{H}_2}+5X_{\mathrm{H_2O}})/(R^o T)$ in terms of the initial mole fractions X_i.

The explicit prediction given in (17) is compared in Figs. 3 and 4 with detailed-chemistry results. In particular, Fig. 3 shows the variation with temperature of the ignition time for a stoichiometric H_2-air mixture, giving excellent agreement for the three pressures tested. As expected, the prediction departs from the detailed-chemistry results as crossover is approached, when (17) predicts $t_i \to 0$ as $\alpha \to 1$, whereas the detailed-chemistry results exhibit the transition towards the fast high-temperature regime. Also, the accuracy degrades somewhat for $p = 50$ atm as the temperature increases above $T \simeq 1200$ K, in the temperature range where the HO_2 steady-state assumption no longer holds, as discussed above in connection with the validity of the 2-step mechanism.

The variation with composition is tested separately in Fig. 4, where results corresponding to H_2-air mixtures at three different pressures are shown, along with results of ignition of H_2-O_2 mixtures at $p = 50$ atm and $p = 500$ atm, two

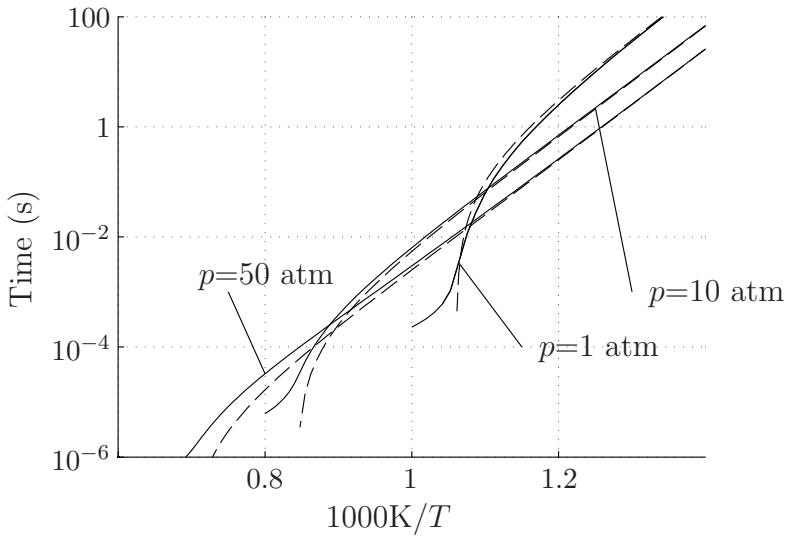

Figure 3: The variation with initial temperature of the ignition time for three different pressures as obtained for a stoichiometric H_2-air mixture by numerical integration of the conservation equations with 21-step chemistry (solid curves) and by evaluation of (17) (dashed curves).

limiting cases bounding the pressure range of interest for cryogenic rocket motor applications. The equivalence ratios investigated extend from very lean to very rich mixtures, within the range of flammability conditions. Except for very lean mixtures at atmospheric pressure, the errors are typically smaller than 20 % for the temperatures selected, i.e., $T = (800, 900, 1000, 1100)$ K for $p = (1, 10, 50, 500)$ atm. Additional computations, not shown in the figure, revealed that the errors are even smaller as the temperature is further decreased, in agreement with the results shown for stoichiometric mixtures in Fig. 3.

For mixtures at atmospheric pressure, the analytic expression tends to overpredict ignition times, giving errors that are more pronounced as the mixture becomes leaner. These overpredictions, exceeding 30 % for $\phi \lesssim 0.2$, are related to one of the simplifications introduced when deriving (6). As

the H_2 concentration decreases for leaner mixtures, the rate of HO_2+H_2 $\stackrel{7}{\rightarrow}$ H_2O_2+H also decreases, which in turn reduces the accuracy of the approximation $(1-\alpha/2)w_7+\alpha w_8 \simeq w_7$ used in writing $\omega_{\rm II}$, because the value of α is not small for these near-crossover conditions (e.g., $\alpha = 0.203$ for $\phi = 0.1$) and the rate w_8 is independent of the H_2 concentration. Clearly, the error decreases rapidly as conditions move away from crossover, so that, for instance, at $\phi = 0.1$ and $p = 1$ atm the overprediction in ignition time is only 8 % when $T = 700$ K. This higher-order effect could be included in the asymptotic development by accounting for the missing term in (11), but that analysis is not pursued further here, because the expected improvements are limited to very lean mixtures near crossover, and the results are not reducible to a simple explicit form, such as that given in (17).

6. Conclusions

This paper has shown how reduced-chemistry techniques based on chemical-time disparities can be combined with activation-energy asymptotics to yield an explicit expression for the ignition time of hydrogen-oxygen mixtures when the initial temperature is below the so-called crossover temperature. This expression shows that, while the rate of the branching step 1 (compared with that of the recombination step 4) becomes important for reducing the ignition time as crossover is approached, far from crossover the induction delay depends instead only on the rate and energetic parameters of the steps 6, 7 and 8, involving H_2O_2, the ignition delay decreasing with increasing rate constants of steps 8 and 7 and (more weakly) with a decreasing rate constant for step 6, according to the power-law factors exhibited in (17). The delay varies inversely with pressure, as is expected from the second-order (binary-collision) chemistry and exhibits effectively a 2/3 reaction-order dependence

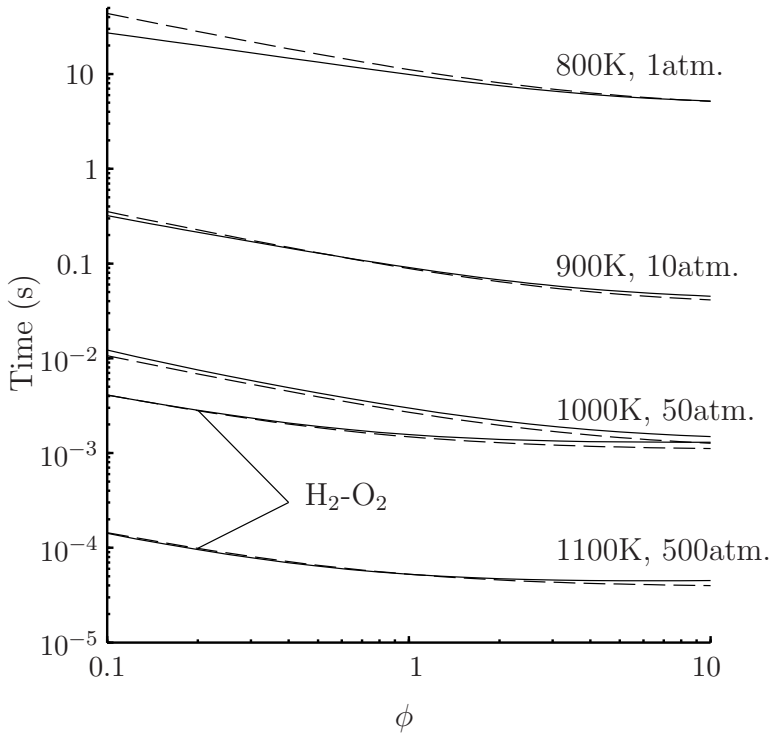

Figure 4: The variation with equivalence ratio of the ignition time as obtained by numerical integration of the conservation equations with 21-step chemistry (solid curves) and by evaluation of (17) (dashed curves) for H_2-air mixtures at different conditions of pressure and initial temperature and also for a H_2-O_2 mixture at $p = 50$ atm and $T = 1000$ K and at $p = 500$ atm and $T = 1100$ K.

on the H_2 concentration, while being independent of the O_2 concentration.

The ignition-delay expression provided here has been tested to predict ignition times with accuracies that are typically better than 20 % over a wide range of temperature, pressures and compositions. Reduced accuracy is found only at elevated pressure for temperatures higher than $T \simeq 1100$ K, arising because of failure of the HO_2 steady-state approximation under those conditions, and also for extremely lean mixtures close to crossover, for which a more elaborate analysis would be needed to account for the greater complexity in the tradeoff between the contributions of steps 7 and 8 to H_2O_2 production and consumption. Nevertheless, the overall performance of the expression proposed for the ignition time is in general very satisfactory.

Acknowledgements

This work was supported by the Comunidad de Madrid through project # P2009/ENE-1597. The first two authors also acknowledge support from the EU through the Marie Curie ITN MYPLANET and from the Spanish MCINN through projects # ENE2008-06515 and CSD2010-00011.

References

[1] G.L. Schott, J.L. Kinsey, J. Chem. Phys. 29 (1958) 1177–1182.

[2] R. Kushida, The reaction of hydrogen and oxygen at high temperature. National Engineering Science Company, Air Force Contract No. AF3396160-8606, 1962.

[3] T. Asaba, W.C. Gardiner, R.F. Stubbeman, Proc. Combust. Inst. 10 (1965) 295–302.

[4] R.R. Graig, A shock-tube study of the ignition delay of hydrogen-air mixtures near the second explosion limit. Report AFAPL-TR-66-74, 1966.

[5] T. Just, F. Schmalz, Measurements of ignition delays of hydrogen-air mixtures under simulated conditions of supersonic combustion chambers. AGARD CP No. 34, Part 2, Paper 19, 1968.

[6] C. Treviño, Ignition phenomena in H_2-O_2 mixtures. Prog. Astronaut. Aeronaut. 131 (1991) 19–43.

[7] G. del Álamo, F.A. Williams, A. L. Sánchez, Combust. Sci. Tech. 176 (2004) 1599–1626.

[8] F.L. Dryer, M. Chaos, Combust. Flame 152 (2008) 293–299.

[9] S.M. Medvedev, G.L. Agafonov, S.V. Khomik, B.E. Gelfand, Combust. Flame 157 (2010) 1436–1438.

[10] P. Saxena, F.A. Williams, Combust. Flame 145 (2006) 316–323. Also available at http://maeweb.ucsd.edu/∼combustion/cermech/.

[11] B. Varatharajan, F.A. Williams, Combust. Flame 121 (2000) 551–554.

	Reaction		A^{a}	n	E^{a}
1	$H+O_2 \rightarrow OH+O$		$3.52\ 10^{16}$	-0.7	71.42
2	$H_2+O \rightarrow OH+H$		$5.06\ 10^{4}$	2.67	26.32
3	$H_2+OH \rightarrow H_2O+H$		$1.17\ 10^{9}$	1.3	15.21
4	$H+O_2+M \rightarrow HO_2+M^{\mathrm{b}}$	k_0	$5.75\ 10^{19}$	-1.4	0.0
		k_∞	$4.65\ 10^{12}$	0.44	0.0
5	$H_2+O_2 \rightarrow HO_2+H$		$2.69\ 10^{12}$	0.36	231.86
6	$2HO_2 \rightarrow H_2O_2+O_2$		$3.02\ 10^{12}$	0.0	5.8
7	$HO_2+H_2 \rightarrow H_2O_2+H$		$1.62\ 10^{11}$	0.61	100.14
8	$H_2O_2+M \rightarrow 2OH+M^{\mathrm{c}}$	k_0	$8.15\ 10^{23}$	-1.9	207.62
		k_∞	$2.62\ 10^{19}$	-1.39	214.74

Table 1: Rate coefficients in Arrhenius form $k = AT^n \exp(-E/R^oT)$ for the skeletal mechanism.

[a] Units are mol, s, cm^3, kJ, and K.

[b] Chaperon efficiencies are 2.5 for H_2, 16.0 for H_2O, 0.7 for Ar and He and 1.0 for all other species; Troe falloff with $F_c = 0.5$

[c] Chaperon efficiencies are 2.0 for H_2, 6.0 for H_2O, 0.4 for Ar and He and 1.0 for all other species; $F_c = 0.265 \exp(-T/94\mathrm{K}) + 0.735 \exp(-T/1756\mathrm{K}) + \exp(-5182\mathrm{K}/T)$